



# **GEOLOGY FOR SOCIETY**

SINCE 1858



**GEOLOGICAL  
SURVEY OF  
NORWAY**

· NGU ·



<b>Report no.:</b> 2021.007		<b>ISSN: 0800-3416 (print)</b> <b>ISSN: 2387-3515 (online)</b>	<b>Grading:</b> Open
<b>Title:</b> Helicopter-borne magnetic, electro-magnetic and radiometric geophysical survey in Treungen and Vegårshei area, Agder, and Vestfold og Telemark counties.			
<b>Authors:</b> Frode Ofstad, Georgios Tassis		<b>Client:</b> NGU	
<b>County:</b> Agder, Vestfold og Telemark		<b>Municipality:</b> Fyresdal, Nissedal, Åmil, Vegårshei, Gjerstad	
<b>Map-sheet name (M=1:250.000)</b> Skien og Arendal		<b>Map-sheet no. and -name (M=1:50.000)</b> 1512-1, 1513-2, 1612-1, 1612-4, 1613-3	
<b>Deposit name and grid-reference:</b> WGS84 UTM32N 475000E, 653000N		<b>Number of pages:</b> 32 <b>Price (NOK):</b> 120 <b>Map enclosures:</b>	
<b>Fieldwork carried out:</b> June-Oct 2020	<b>Date of report:</b> March 2021	<b>Project no.:</b> 388900	<b>Person responsible:</b> 

**Summary:**

NGU conducted an airborne geophysical survey in Fyresdal, Nissedal, Åmil, Vegårshei, Gjerstad municipalities as part of NGU's general airborne mapping program. Treungen area was completed in June 2020, and Vegårshei area completed in October 2020.

This report describes and documents the acquisition, processing and visualization of the acquired datasets and presents them in maps. The geophysical surveys consist of 5500 line-km data, covering an area of 1100 km<sup>2</sup>, with 2930 km (586 km<sup>2</sup>) flown in June from Gautefall, and 2570 km (514 km<sup>2</sup>) flown in September/October from Ubergsmoen.

The NGU modified Geotech Ltd. Hummingbird frequency domain EM system supplemented by an optically pumped Cesium magnetometer and the Radiation Solutions 1024 channels RSX-5 spectrometer mounted on a AS350-B3 helicopter was used for data acquisition.

The survey was flown with 200 meters line spacing, azimuth 90°. Average speed was 110 km/h, and average height clearance of the EM bird was 57m and 87m for the spectrometer.

Collected data were processed at NGU using Geosoft Oasis Montaj software. Raw total magnetic field data were corrected for diurnal variation and leveled using standard micro levelling algorithm. Radiometric data were processed using standard procedures recommended by International Atomic Energy Association (IAEA).

EM data were filtered and leveled using both automated and manual levelling procedures. Apparent resistivity was calculated from in-phase and quadrature data for three coplanar frequencies (880Hz, 6.6kHz and 34kHz), and for two coaxial frequencies (980Hz and 7kHz) separately using a homogeneous half space model.

All data were gridded using cell size of 50x50 meters and presented as 40% transparent grids with shaded relief on top of topographic maps.

<b>Keywords:</b>	<b>Airborne</b>	<b>Geophysics</b>
<b>Magnetic</b>	<b>Gamma spectrometry</b>	<b>Radiometric</b>
<b>Electromagnetic</b>	<b>Technical report</b>	

## CONTENTS

<b>1. SURVEY SPECIFICATIONS</b> .....	<b>5</b>
1.1 Airborne Survey Parameters .....	5
1.2 Airborne Survey Instrumentation.....	6
1.3 Airborne Survey Logistics Summary .....	7
<b>2. DATA PROCESSING AND PRESENTATION</b> .....	<b>8</b>
2.1 Total Field Magnetic Data .....	8
2.2 Electromagnetic Data .....	10
2.3 Radiometric data.....	11
<b>3. PRODUCTS</b> .....	<b>15</b>
<b>4. REFERENCES</b> .....	<b>15</b>
Appendix A1: Flow chart of magnetic processing.....	16
Appendix A2: Flow chart of EM processing .....	16
Appendix A3: Flow chart of radiometry processing.....	16

## FIGURES

Figure 1: Helicopter survey areas in Agder, Vestfold og Telemark.....	4
Figure 2: Hummingbird system in air .....	7
Figure 3: Gamma-ray spectrum with K, Th, U and Total Count windows.....	11
Figure 4: Treungen and Vegårshei survey areas with flight path .....	18
Figure 5: Total Magnetic Field .....	19
Figure 6: Magnetic Horizontal Gradient .....	20
Figure 7: Magnetic Vertical Derivative.....	21
Figure 8: Magnetic Tilt Derivative .....	22
Figure 9: Apparent resistivity. Frequency 7000 Hz, Coaxial coils .....	23
Figure 10: Apparent resistivity. Frequency 6600 Hz, Coplanar coils .....	24
Figure 11: Apparent resistivity. Frequency 980 Hz, Coaxial coils .....	25
Figure 12: Apparent resistivity. Frequency 880 Hz, Coplanar coils .....	26
Figure 13 Apparent resistivity. Frequency 34133 Hz, Coplanar coils .....	27
Figure 14: Radiometric Total counts.....	28
Figure 15: Potassium ground concentration .....	29
Figure 16: Uranium ground concentration .....	30
Figure 17: Thorium ground concentration .....	31
Figure 18: Radiometric Ternary Image .....	32

## TABLES

Table 1. Flight specifications .....	5
Table 2. Instrument Specifications .....	6
Table 3. Hummingbird EM system, frequency and coil configurations .....	7
Table 4. Survey Specifications Summary .....	7
Table 5. Specified channel windows for the 1024 RSX-5 system. ....	11
Table 6. Maps in scale 1:100.000, available from NGU on request.....	15

## INTRODUCTION

In 2020 NGU received government funds to acquire airborne geophysical data from parts of Agder and Telemark counties. The surveyed area is situated between Fyresvatnet in the west, Gautefall in the east, and Åmli in the south. The helicopter survey reported herein amounts to 5500 line-km, or 1100 km<sup>2</sup>, with areas covered shown in Figure 1. The Treungen area, flown in June, is marked with an orange border, and the Vegårshei area, flown in September/October, is marked with a red border.

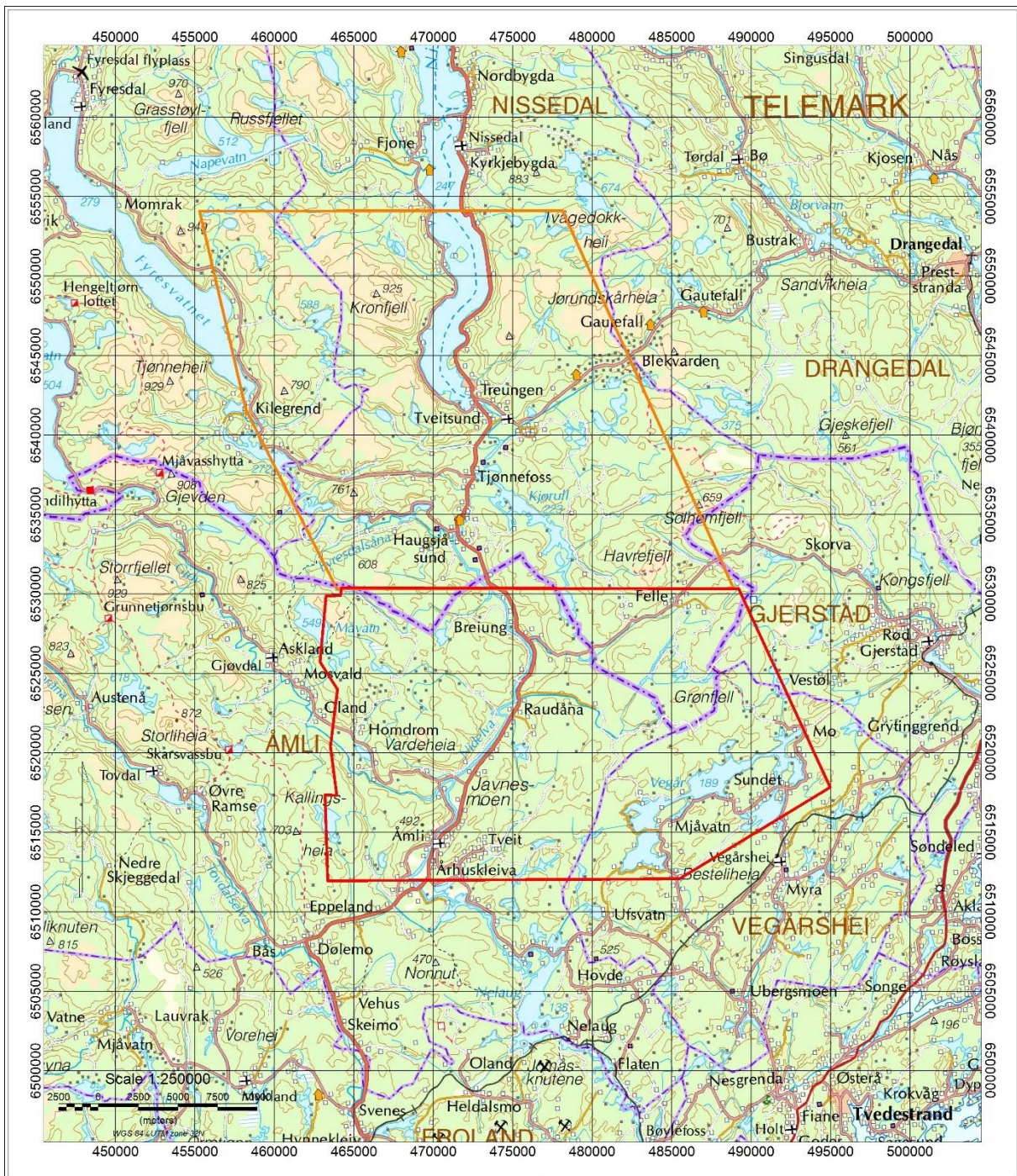


Figure 1: Helicopter survey areas in Agder, Vestfold og Telemark.

**Table 1. Flight specifications**

Survey Name	Surveyed lines (km)	Surveyed area (Km <sup>2</sup> )	Flight direction	Average flight speed (km/h)
Treungen 2020	2930	586	90	115
Vegårshei 2020	2570	514	90	108

The objective of the airborne geophysical survey was to obtain a dense high-resolution magnetic, electro-magnetic and radiometric data set over the survey area. This data is required for the enhancement of a general understanding of the regional geology of the area, with adjoining areas covered by other airborne surveys earlier years.

In this regard, the new data can be used to map contacts and structural features within the survey area. It also improves defining the potential of known zones of mineralization, their geological settings, and identifying new areas of interest, as the dataset fills a gap in the high-resolution geophysical surveys of the region.

The survey incorporated the use of a Hummingbird™ 5-frequency electromagnetic system supplemented by a high-sensitivity cesium magnetometer, gamma-ray spectrometer, and radar altimeter. A GPS navigation computer system with flight path indicators ensured accurate positioning of the geophysical data with respect to the World Geodetic System 1984 geodetic datum (WGS-84).

## 1. SURVEY SPECIFICATIONS

### 1.1 Airborne Survey Parameters

NGU used a modified Hummingbird™ electromagnetic and magnetic helicopter survey system designed to obtain low level, slow speed, detailed airborne magnetic and electromagnetic data (Geotech 1997). The system was supplemented by 1024 channel gamma-ray spectrometer, installed under the belly of the helicopter, which was used to map ground concentrations of U, Th and K, and radiation Total Counts.

The airborne survey began on June 3<sup>rd</sup>, 2020 and ended on October 8<sup>th</sup>, 2020. A Eurocopter AS350-B3 (LN-OSD) from helicopter company Pegasus Helicopter AS was used to tow the bird. The survey lines were spaced 200 meters apart, with lines oriented at 90°. The magnetic and electromagnetic sensors are housed in a single 7 meters long bird, flown at an average of about 57 m above the topographic surface.

Rugged terrain and abrupt changes in topography affected the aircraft pilot's ability to 'drape' the terrain, meaning the average instrumental height was sometimes higher than the standard survey instrumental height, which is defined as 30 meters plus a height of obstacles (trees, power lines etc.) for EM and magnetic sensors.

The ground speed of the aircraft varied from 50 – 140 km/h depending on topography, wind direction and its magnitude. On average the ground speed during measurements is calculated to 110 km/h. Magnetic data were recorded at 0.2 second intervals resulting in approximately 6 meters average point spacing.

EM data were recorded at 0.1 second intervals resulting in data with a sample increment of 3 meters along the ground in average. Spectrometry data were recorded every 1 second giving a point spacing of approximately 30 meters. The above

parameters allow recognizing sufficient detail in the data to detect subtle anomalies that may represent mineralization and/or rocks of different lithological and petrophysical composition.

A base magnetometer to monitor diurnal variations in the magnetic field was located at the base, in June at Gautefall, and Ubergsmoen in September/October. The GEM GSM-19 station magnetometer data were recorded once every 3 seconds. The CPU clock of the base magnetometer and the helicopter magnetometer were both synchronized to UTC (Universal Time Coordinates) through the built-in GPS receiver to allow correction of diurnals.

Navigation system uses GPS/GLONASS satellite tracking systems to provide real-time WGS-84 coordinate locations for every second. The accuracy achieved with no differential corrections is reported to be  $\pm 5$  meters in the horizontal directions. The GPS receiver antenna was mounted internally inside the canopy of the helicopter.

For quality control, the electromagnetic, magnetic, and radiometric, altitude and navigation data were monitored on four separate windows in the operator's display during flight while they were recorded in three data ASCII streams to the PC hard disk drive. Spectrometry data were also recorded to an internal hard drive of the spectrometer. The data files were transferred to the field workstation via USB flash drive. The raw data files were backed up onto USB flash drive in the field.

## 1.2 Airborne Survey Instrumentation

Instrument specification is given in Table 2. Frequencies and coil configuration for the Hummingbird EM system is given in Table 3.

**Table 2. Instrument Specifications**

<b>Instrument</b>	<b>Producer/Model</b>	<b>Accuracy / Sensitivity</b>	<b>Sampling frequency / interval</b>
Magnetometer	Scintrex Cs-2	<2.5nT throughout range / 0.0006nT $\sqrt{\text{Hz}}$ rms	5 Hz
Base magnetometer	GEM GSM-19	0.1 nT	3 s
Electromagnetic	Geotech Hummingbird	1 – 2 ppm	10 Hz
Gamma spectrometer	Radiation Solutions RSX-5	1024 ch's, 16 liters down, 4 liters up	1 Hz
Radar altimeter	Bendix/King KRA 405B	$\pm 3\%$ 0 – 500 feet $\pm 5\%$ 500 – 2500 feet	1 Hz
Pressure/temperature	Honeywell PPT	$\pm 0.03\%$ FS	1 Hz
Navigation	Topcon GPS-receiver	$\pm 5$ meter	1 Hz
Acquisition system	NGU custom software		

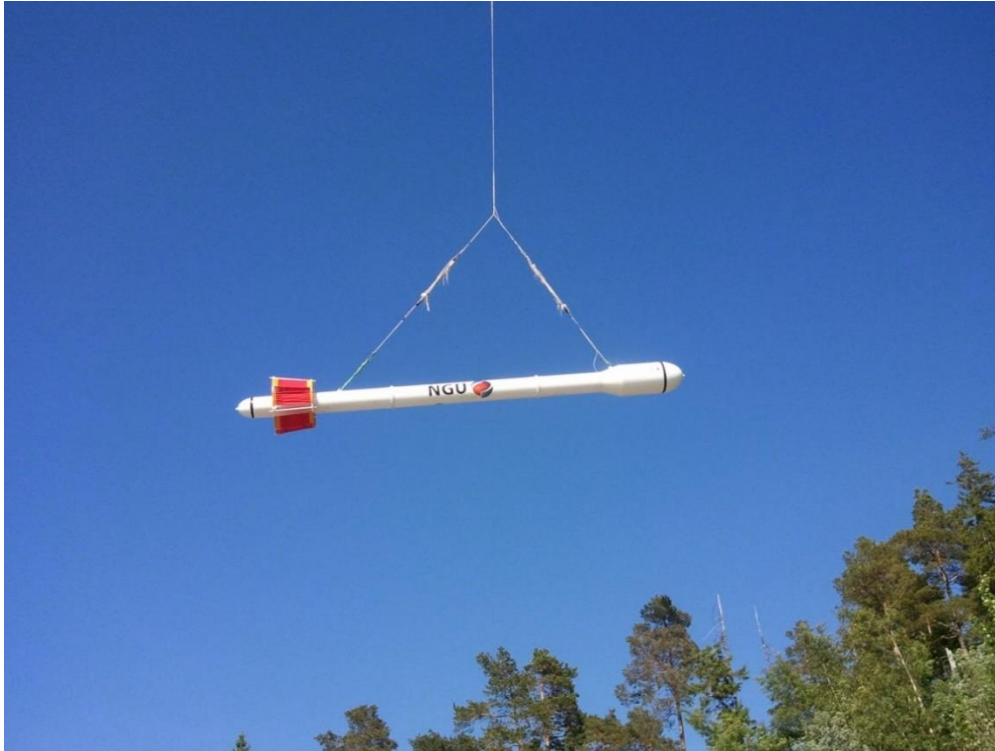


Figure 2: Hummingbird system in air

Table 3. Hummingbird EM system, frequency and coil configurations

Coils	Frequency	Orientation	Separation
A	7700 Hz	Coaxial	6.30 m
B	6600 Hz	Coplanar	6.30 m
C	980 Hz	Coaxial	6.025 m
D	880 Hz	Coplanar	6.025 m
E	34133 Hz	Coplanar	4.90 m

### 1.3 Airborne Survey Logistics Summary

A summary of the survey specifications is shown in Table 4.

Table 4. Survey Specifications Summary

Parameter	Specifications
Traverse (survey) line spacing	200 meters
Traverse line direction	E-W (90°)
Nominal aircraft ground speed	70 - 120 km/h
Average aircraft ground speed	110 km/h
Average sensor terrain clearance Mag	57 meters
Average sensor terrain clearance Rad	87 meters
Sampling rates:	
Magnetometer	0.2 seconds
EM	0.1 seconds
Spectrometer, GPS, altimeter	1.0 second
Base Magnetometer	3.0 seconds

## 2. DATA PROCESSING AND PRESENTATION

The new magnetic, spectrometry and all resistivity data were processed by Frode Ofstad at NGU. The ASCII data files were loaded into three separate Oasis Montaj databases. All three datasets were processed consequently according to processing flow charts shown in Appendix A1, A2 and A3.

### 2.1 Total Field Magnetic Data

At the first stage the raw magnetic data was visually inspected, and spikes were removed manually. Non-linear filter was also applied to airborne raw data to eliminate short-period spikes. Typically, several corrections must be applied to magnetic data before gridding - heading correction, lag correction and diurnal correction.

#### Diurnal Corrections

The temporal fluctuations in the magnetic field of the earth affect the total magnetic field readings recorded during the airborne survey. This is commonly referred to as the magnetic diurnal variation. These fluctuations can be effectively removed from the airborne magnetic dataset by using a stationary reference magnetometer that records the magnetic field of the earth simultaneously with the airborne sensor at given short time interval.

Diurnal variation channel was inspected for spikes, and spikes were removed manually if necessary. Magnetic diurnals that were recorded on the base station magnetometer were within the standard NGU specifications during the entire survey (Rønning 2013).

Diurnal variations were measured with GEM GSM-19 magnetometer. The base station computer clock was continuously synchronized with GPS clock. The recorded data are merged with the airborne data and the diurnal correction is applied according to equation (1).

$$\mathbf{B}_{Tc} = \mathbf{B}_T + (\bar{B}_B - \mathbf{B}_B), \quad (1)$$

Where:

$\mathbf{B}_{Tc}$  = Corrected airborne total field readings

$\mathbf{B}_T$  = Airborne total field readings

$\bar{B}_B$  = Averaged datum base level

$\mathbf{B}_B$  = Base station readings

The average datum base level ( $\bar{B}_B$ ) was set to 50936 nT for the Treungen survey, flown in June, and at 50420 nT for Vegårshei area, flown in September/October.

#### Corrections for Lag and heading

Neither a lag nor cloverleaf tests were performed before the survey. According to previous reports the lag between logged magnetic data and the corresponding navigational data was 1-2 fids. Translated to a distance it would be no more than 10 meter - the value comparable with the precision of GPS. A heading error for a towed system is usually either very small or non-existent. No lag and heading corrections were applied.



### Magnetic data processing, gridding, and presentation

The total field magnetic anomaly data ( $\mathbf{B}_{TA}$ ) were calculated from the diurnal corrected data ( $\mathbf{B}_{Tc}$ ) after subtracting the IGRF for the surveyed area calculated for the data period (eq.2)

$$\mathbf{B}_{TA} = \mathbf{B}_{Tc} - IGRF \quad (2)$$

IGRF 2015 model was employed in these calculations, to ensure that the Treungen and Vegårshei data would match the previously processed and earlier published surrounding data sets, from Drangedal and Telemark.

The total field anomaly data were split into lines and then were gridded using a minimum curvature method with a grid cell size of 50 meters. This cell size is exactly one quarter of the 200 meters average line spacing. To remove small line-to-line levelling errors that were detected on the gridded magnetic anomaly data, the Geosoft micro-levelling technique was applied on the flight line based magnetic database. Then, the micro-leveled channel was gridded using minimum curvature method with 50 meters grid cell size.

The processing steps of magnetic data presented so far, were performed on point basis. The following steps are performed on grid basis.

The horizontal and vertical gradient along with the tilt derivative of the total magnetic anomaly were calculated from the stitched micro-leveled total magnetic anomaly grid. The magnitude of the horizontal gradient was calculated according to equation (3)

$$HG = \sqrt{\left(\frac{\partial(\mathbf{B}_{TA})}{\partial x}\right)^2 + \left(\frac{\partial(\mathbf{B}_{TA})}{\partial y}\right)^2} \quad (3)$$

where  $\mathbf{B}_{TA}$  is the micro-leveled total field anomaly field. The vertical gradient (VG) was calculated by applying a vertical derivative convolution filter to the micro-leveled  $\mathbf{B}_{TA}$  field. The tilt derivative (TD) was calculated according to the equation (4)

$$TD = \tan^{-1}\left(\frac{VG}{HG}\right) \quad (4)$$

A 3x3 convolution filter was applied to smooth the resulted magnetic grids.

The results are presented in a series of colored shaded relief maps (1:100.000). The maps are:

- A. Total field magnetic anomaly
- B. Horizontal gradient of total magnetic anomaly
- C. Vertical gradient of total magnetic anomaly
- D. Tilt derivative (or Tilt angle) of the total magnetic anomaly

These maps are representative of the distribution of magnetization over the surveyed areas. The list of the produced maps is shown in Table 6.

## 2.2 Electromagnetic Data

The EM system transmits five fixed frequencies and records an in-phase and a quadrature response for each of the five coil sets of the electromagnetic system. The received signals are processed and used for computation of an apparent resistivity.

In-phase and quadrature data were filtered with 15 fiducial non-linear filter to eliminate spherical spikes, which were represented as irregular noise of large amplitude in records and high frequency noise of bird electronics. Then, a 20-fiducial low-pass filter was applied to suppress instrumental and cultural noise. These filters were not able to suppress all the noise. Also, shifts of 7000 IP and Q records, with amplitude of 5-10 ppm, was observed in some flights. Shifts were edited manually where possible.

To remove the effects of instrument drift caused by gradual temperature variations in the transmitting and receiving circuits, background responses are recorded during each flight. To obtain a background level, the bird is raised to an altitude of at least 1000 ft above the topographic surface so that no electromagnetic responses from the ground are present in the recorded traces.

The EM traces observed at this altitude correspond to a background (zero) level of the system. If these background levels are recorded at 20-30 minutes interval, then the linear drift of the system can be removed on a flight-by-flight basis, before any further processing is carried out. Geosoft HEM module was used for applying drift correction. Residual instrumental drift, usually small, but non-linear, was manually removed on a line-to-line basis.

When levelling of the EM data was complete, apparent resistivity was calculated from in-phase and quadrature EM components using a homogeneous half space model of the earth (Geosoft HEM module) for 6600, 7000, 980, 880 and 34133 Hz. A threshold value of 3 ppm was set for inversion, with a starting value of 500 ohm-m.

Electromagnetic field decays rapidly with the distance (height of the sensors) – as  $z^{-2}$  –  $z^{-5}$  depending on the shape of the conductors and, at certain height, signals from the ground sources become comparable with instrumental noise. Levelling errors or precision of levelling can lead sometimes to appearance of artificial resistivity anomalies when data were collected at high instrumental altitude.

Application of threshold allows excluding such data from an apparent resistivity calculation, though not completely. It is particularly noticeable in low frequencies datasets. Resistivity data were visually inspected; artificial anomalies associated with high altitude measurements were manually removed.

For better visual appearance of the data, proxy resistivity values between 1 to 13 was used:  $<3\Omega=1$ ,  $3-5\Omega=2$ ,  $5-10\Omega=3$ ,  $10-20\Omega=4$ ,  $20-50\Omega=5$ ,  $50-100\Omega=6$ ,  $100-200\Omega=7$ ,  $200-500\Omega=8$ ,  $500-1000\Omega=9$ ,  $1000-2000\Omega=10$ ,  $2000-5000\Omega=11$ ,  $5000-10000\Omega=12$ ,  $>10000\Omega=13$ . This gridding method produces smoother maps with fewer artefacts.

Data recorded at the height above 150 meters were considered as non-reliable and removed from presentation. Proxy resistivity were gridded with a cell size 50 meters. Power lines strongly affected low frequency data – 880 and 980 Hz channels, and the most prominent noise from power lines were filtered manually.

### 2.3 Radiometric data

Airborne gamma-ray spectrometry measures the abundance of Potassium (K), Thorium (eTh), and Uranium (eU) in rocks and weathered materials by detecting gamma-rays emitted due to the natural radioelement decay of these elements. The data analysis method is based on the IAEA recommended method for U, Th and K (International Atomic Energy Agency, 1991; 2003). A short description of the individual processing steps of that methodology as adopted by NGU is given below.

#### Energy windows

The Gamma-ray spectra were initially reduced into standard energy windows corresponding to the individual radio-nuclides K, U and Th. Figure 3 shows an example of a Gamma-ray spectrum and the corresponding energy windows and radioisotopes (with peak energy in MeV) responsible for the radiation.

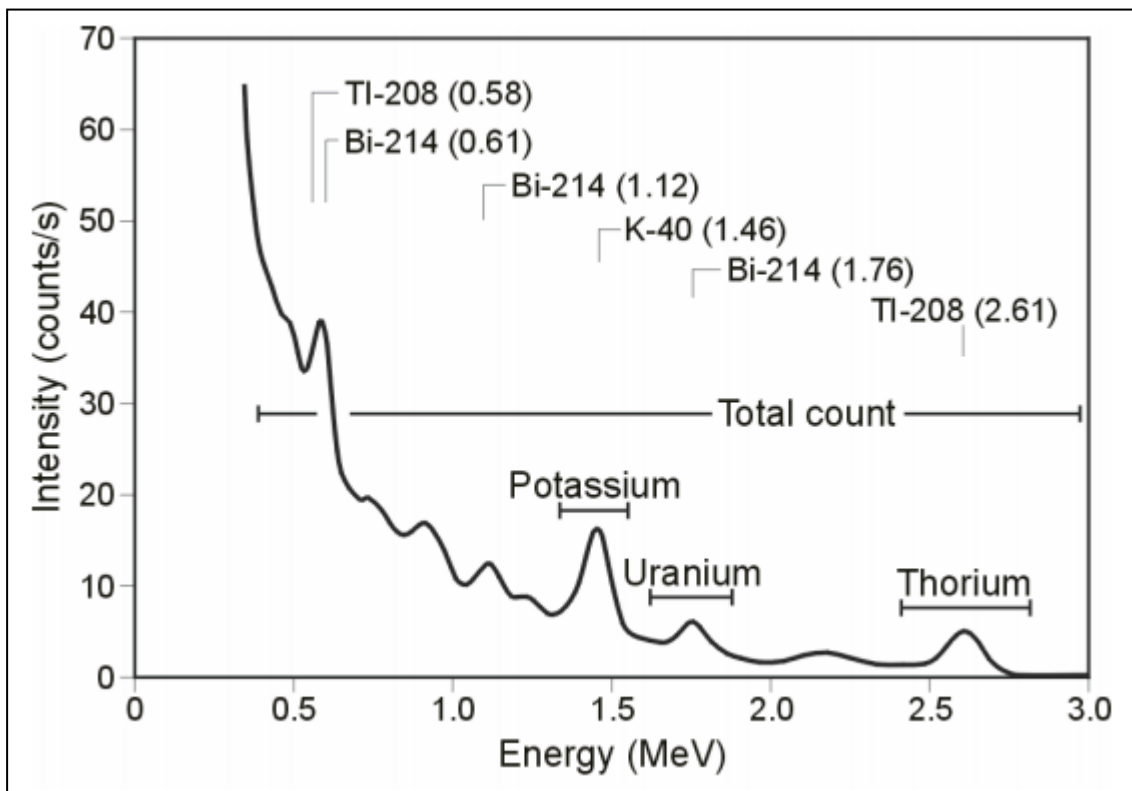


Figure 3: Gamma-ray spectrum with K, Th, U and Total Count windows.

Table 5. Specified channel windows for the 1024 RSX-5 system.

Gamma-ray spectrum	Cosmic	Total count	K	U	Th
Down	1023	136-937	456-522	552-619	802-936
Up	1023			552-619	
Energy windows (MeV)	>3.07	0.41-2.81	1.37-1.57	1.66-1.86	2.41-2.81

The RSX-5 is a 1024 channel system with four downward and one upward looking detector, which means that the actual Gamma-ray spectrum is divided into 1024 channels. The first channel is reserved for the “Live Time” and the last for the Cosmic rays. Table 5 shows the channels that were used for the reduction of the spectrum.

### Live Time correction

The data were corrected for live time. “Live time” is an expression of the relative length of time the instrument was able to register new pulses per sample interval. On the other hand, “dead time” is an expression of the relative length of time the system was unable to register new pulses per sample interval. The relation between “dead time” and “live time” is given by the equation (5)

$$\text{“Live time”} = \text{“Real time”} - \text{“Dead time”} \quad (5)$$

where the “real time” or “acquisition time” is the elapsed time over which the spectrum is accumulated (about 1 second).

The live time correction is applied to the total count, Potassium, Uranium, Thorium, upward Uranium, and cosmic channels. The formula used to apply the correction is as follows:

$$C_{LT} = C_{RAW} \cdot \frac{\text{Acquisition Time}}{\text{Live Time}} \quad (6)$$

where  $C_{LT}$  is the live time corrected channel in counts per second,  $C_{RAW}$  is the raw channel data in counts per second, while Acquisition Time and Live Time are in microseconds.

### Cosmic and aircraft correction

Background radiation resulting from cosmic rays and aircraft contamination was removed from the total count, Potassium, Uranium, Thorium, upward Uranium channels using the following formula:

$$C_{CA} = C_{LT} - (a_c + b_c \cdot C_{Cos}) \quad (7)$$

where  $C_{CA}$  is the cosmic and aircraft corrected channel,  $C_{LT}$  is the live time corrected channel  $a_c$  is the aircraft background for this channel,  $b_c$  is the cosmic stripping coefficient for this channel and  $C_{Cos}$  is the low pass filtered cosmic channel.

### Radon correction

The upward detector method, as discussed in IAEA (1991), was applied to remove the effects of the atmospheric radon in the air below and around the helicopter. Using spectrometry data over-water, where there is no contribution from the ground sources, enables the calculation of the coefficients ( $a_c$  and  $b_c$ ) for the linear equations that relate the cosmic corrected counts per second of Uranium channel with that of total count, Potassium, Thorium and Uranium upward channels over water. Data over-land was used in conjunction with data over-water to calculate the  $a_1$  and  $a_2$  coefficients used in equation (8) for the determination of the Radon component in the downward uranium window:

$$Radon_U = \frac{U_{up_{CA}} - a_1 \cdot U_{CA} - a_2 \cdot Th_{CA} + a_2 \cdot b_{Th} - b_U}{a_U - a_1 - a_2 \cdot a_{Th}} \quad (8)$$

where  $Radon_U$  is the radon component in the downward Uranium window,  $U_{up_{CA}}$  is the filtered upward uranium,  $U_{CA}$  is the filtered Uranium,  $Th_{CA}$  is the filtered Thorium,  $a_1$ ,  $a_2$ ,  $a_U$  and  $a_{Th}$  are proportional factors and  $b_U$  and  $b_{Th}$  are constants determined experimentally.

The effects of Radon in the downward Uranium are removed by simply subtracting Radon<sub>U</sub> from U<sub>CA</sub>. The effects of radon in the other channels are removed using the following formula:

$$C_{RC} = C_{CA} - (a_C \cdot \text{Radon}_U + b_C) \quad (9)$$

where C<sub>RC</sub> is the Radon corrected channel, C<sub>CA</sub> is the cosmic and aircraft corrected channel, Radon<sub>U</sub> is the Radon component in the downward uranium window, a<sub>C</sub> is the proportionality factor and b<sub>C</sub> is the constant determined experimentally for this channel from over-water data.

### Compton Stripping

Potassium, Uranium and Thorium Radon corrected channels, are subjected to spectral overlap correction. Compton scattered gamma rays in the radio-nuclides energy windows were corrected by window stripping using Compton stripping coefficients determined from measurements on calibrations pads (Grasty et al, 1991) at the Geological Survey of Norway in Trondheim (see values in Appendix A2).

The stripping corrections are given by the following formulas:

$$A_1 = 1 - (g \cdot \gamma) - (a \cdot \alpha) + (a \cdot g \cdot \beta) - (b \cdot \beta) + (b \cdot \alpha \cdot \gamma) \quad (10)$$

$$U_{ST} = \frac{Th_{RC} \cdot ((g \cdot \beta) - \alpha) + U_{RC} \cdot (1 - b \cdot \beta) + K_{RC} \cdot ((b \cdot \alpha) - g)}{A_1} \quad (11)$$

$$Th_{ST} = \frac{Th_{RC} \cdot (1 - (g \cdot \gamma)) + U_{RC} \cdot (b \cdot \gamma - a) + K_{RC} \cdot ((a \cdot g) - b)}{A_1} \quad (12)$$

$$K_{ST} = \frac{Th_{RC} \cdot ((\alpha \cdot \gamma) - \beta) + U_{RC} \cdot ((a \cdot \beta) - \gamma) + K_{RC} \cdot (1 - (a \cdot \alpha))}{A_1} \quad (13)$$

where U<sub>RC</sub>, Th<sub>RC</sub>, K<sub>RC</sub> are the radon corrected Uranium, Thorium and Potassium and a, b, g, α, β, γ are Compton stripping coefficients. U<sub>ST</sub>, Th<sub>ST</sub> and K<sub>ST</sub> are stripped values of U, Th and K.

### Reduction to Standard Temperature and Pressure

The radar altimeter data were converted to effective height (H<sub>STP</sub>) using the acquired temperature and pressure data, according to the expression:

$$H_{STP} = H \cdot \frac{273.15}{T + 273.15} \cdot \frac{P}{1013.25} \quad (14)$$

where H is the smoothed observed radar altitude in meters, T is the measured air temperature in degrees Celsius and P is the measured barometric pressure in millibars.

### Height correction

Variations caused by changes in the aircraft altitude relative to the ground was corrected to a nominal height of 60 m. Data recorded at the height above 150 m were considered as non-reliable and removed from processing. Total count, Uranium, Thorium and Potassium stripped channels were subjected to height correction according to the equation:

$$C_{60m} = C_{ST} \cdot e^{C_{hi} \cdot (60 - H_{STP})} \quad (15)$$

where  $C_{ST}$  is the stripped corrected channel,  $C_{ht}$  is the height attenuation factor for that channel and  $H_{STP}$  is the effective height.

### **Conversion to ground concentrations**

Finally, corrected count rates were converted to effective ground element concentrations using calibration values derived from calibration pads (Grasty et al, 1991) at the Geological Survey of Norway in Trondheim (see values in Appendix A2). The corrected data provide an estimate of the apparent surface concentrations of Potassium, Uranium and Thorium (K, eU and eTh). Potassium concentration is expressed as a percentage, equivalent Uranium and Thorium as parts per million (ppm). Uranium and Thorium are described as “equivalent” since their presence is inferred from gamma-ray radiation from daughter elements ( $^{214}\text{Bi}$  for Uranium,  $^{208}\text{Tl}$  for Thorium). The concentration of the elements is calculated according to the following expressions:

$$C_{CONC} = C_{60m} / C_{SENS\_60m} \quad (16)$$

where  $C_{60m}$  is the height corrected channel,  $C_{SENS\_60m}$  is experimentally determined sensitivity reduced to the nominal height (60m).

### **Spectrometry data gridding and presentation**

Gamma-rays from Potassium, Thorium and Uranium emanate from the uppermost 30 to 40 centimeters of soil and rock in the crust (Minty, 1997). Variations in the concentrations of these radioactive elements are largely related to changes in the mineralogy and geochemistry of the Earth’s surface.

The spectrometry data were stored in a database and the ground concentrations were calculated following the processing steps. A list of the parameters used in these steps is given in Appendix A3.

Then the data were split in lines and ground concentrations of the three main natural radio-elements Potassium, Thorium and Uranium and total gamma-ray flux (total count) were gridded using a minimum curvature method with a grid cell size of 50 meters. To remove small line-to-line levelling errors appeared on those grids, the data were micro-leveled as in the case of the magnetic data, and re-gridded with the same grid cell size.

Quality of the radiometric data was within standard NGU specifications (Rønning 2013). For further reading regarding standard processing of airborne radiometric data, we recommend the publications from Minty et al. (1997).

A 3x3 convolution filter was applied to smooth the concentration grids. A list of the produced maps is shown on Table 6.

### 3. PRODUCTS

Processed digital data from the survey are presented as:

1. Geosoft XYZ files: Treungen\_Vegarshei\_Mag.xyz, Treungen\_Vegarshei\_EM.xyz, Treungen\_Vegarshei\_Rad.xyz, Coloured maps at the scale 1:100.000 available from NGU on request.
2. Grid-files in Geotiff format

**Table 6. Maps in scale 1:100.000, available from NGU on request.**

Map #	Name
2021.007-00	Survey Flight Path
2021.007-01	Total magnetic field
2021.007-02	Magnetic Horizontal Gradient
2021.007-03	Magnetic Vertical Gradient
2021.007-04	Magnetic Tilt Derivative
2021.007-05	Apparent resistivity, Frequency 7000 Hz, coaxial coils
2021.007-06	Apparent resistivity, Frequency 6600 Hz, coplanar coils
2014.060-07	Apparent resistivity, Frequency 980 Hz, coaxial coils
2021.007-08	Apparent resistivity, Frequency 880 Hz, coplanar coils
2021.007-09	Apparent resistivity, Frequency 34133 Hz, coplanar coils
2021.007-10	Radiometric Total counts
2021.007-11	Potassium ground concentration
2021.007-12	Uranium ground concentration
2021.007-13	Thorium ground concentration
2021.007-14	Radiometric Ternary Map

Downscaled images of the maps are shown on figures 4 to 17.

### 4. REFERENCES

IAEA 1991: Airborne Gamma-Ray Spectrometry Surveying, Technical Report No 323, Vienna, Austria, 97 pp

Geotech 1997: Hummingbird Electromagnetic System. User manual. Geotech Ltd. October 1997

Grasty, R.L., Holman, P.B. & Blanchard 1991: Transportable Calibration pads for ground and airborne Gamma-ray Spectrometers. Geological Survey of Canada. Paper 90-23. 62 pp.

IAEA 2003: Guidelines for radioelement mapping using gamma ray spectrometry data. IAEA-TECDOC-1363, Vienna, Austria. 173 pp.

Minty, B.R.S., Luyendyk, A.P.J. and Brodie, R.C. 1997: Calibration and data processing for gamma-ray spectrometry. AGSO – Journal of Australian Geology & Geophysics. 17(2). 51-62.

Naudy, H. and Dreyer, H. 1968: Non-linear filtering applied to aeromagnetic profiles. Geophysical Prospecting. 16(2). 171-178.

Rønning, J.S. 2013: NGUs helikoptermålinger. Plan for sikring og kontroll av datakvalitet. NGU Intern rapport 2013.001, (38 sider).

## Appendix A1: Flow chart of magnetic processing

Meaning of parameters is described in the referenced literature.

Processing flow:

- Quality control.
- Visual inspection of airborne data and manual spike removal
- Merge basemag data with EM database
- Import of diurnal data.
- Correction of data for diurnal variation
- IGRF removed.
- Splitting flight data by lines
- Gridding
- Microlevelling
- 3x3 convolution filter

## Appendix A2: Flow chart of EM processing

Meaning of parameters is described in the referenced literature.

Processing flow:

- Filtering of in-phase and quadrature channels with non-linear and low pass filters
- Automated leveling
- Quality control
- Visual inspection of data.
- Splitting flight data by lines
- Manual removal of remaining part of instrumental drift
- Calculation of an apparent resistivity using both - in-phase and quadrature channels.
- Gridding

## Appendix A3: Flow chart of radiometry processing

Underlined processing stages are not only applied to the K, U and Th window, but also to the total count. Meaning of parameters is described in the referenced literature.

- Airborne and cosmic correction (IAEA, 2003)  
Used parameters: determined by high altitude calibration flights (1500-9000 ft) at Langøya in 2013.

Channel	Background	Cosmic
K	8	0.0575
U	1	0.0471
Th	0	0.0638
Uup	0.3926	0.0107
Total counts	37	1.0236



- Radon correction using upward detector method (IAEA, 2003)

Used parameters determined from survey data over water and land at Treungen, June 2020:

Coefficient	Value	Coefficient	Value
$a_u$	0.23956	$b_u$	0.86745
$a_K$	0.7491	$b_K$	0.0
$a_{Th}$	0.04508	$b_{Th}$	0.0
$a_{TC}$	12.61407	$b_{TC}$	11.27617
$a_1$	0.08616792	$a_2$	0.00242527

Used parameters determined from survey data at Vegårshei, October 2020

Coefficient	Value	Coefficient	Value
$a_u$	0.37369	$b_u$	0.0
$a_K$	0.68778	$b_K$	1.43907
$a_{Th}$	0.13992	$b_{Th}$	0.11402
$a_{TC}$	15.44253	$b_{TC}$	8.46545
$a_1$	0.09171662	$a_2$	0.00034295

- Stripping corrections (IAEA, 2003)

Used parameters determined from measurements on calibrations pads at NGU, May 2020

Coefficient	Value
a	0.048088
b	0
c	0
$\alpha$	0.30396
$\beta$	0.475485
$\gamma$	0.825938

- Height correction to a height of 60 m

Parameters determined by high altitude calibration flights (100 – 700 ft). The average values from tests performed at Beitostølen, 2015 were used. Attenuation factors in 1/m:

Channel	Attenuation factor
K	-0.010179
U	-0.008477
Th	-0.008301
TC	-0.009447

- Converting counts at 60 m heights to element concentration on the ground

Used parameters determined from measurements on calibrations pads at NGU, May 2020

Channel	Sensitivity
K (%/count)	0.00764
U (ppm/count)	0.08849
Th (ppm/count)	0.15301

- Microlevelling using Geosoft menu and smoothening by a convolution filtering.

Microlevelling parameters	Value
De-corrugation cutoff wavelength (m)	1200
Cell size for gridding (m)	50
Naudy (1968) Filter length (m)	800

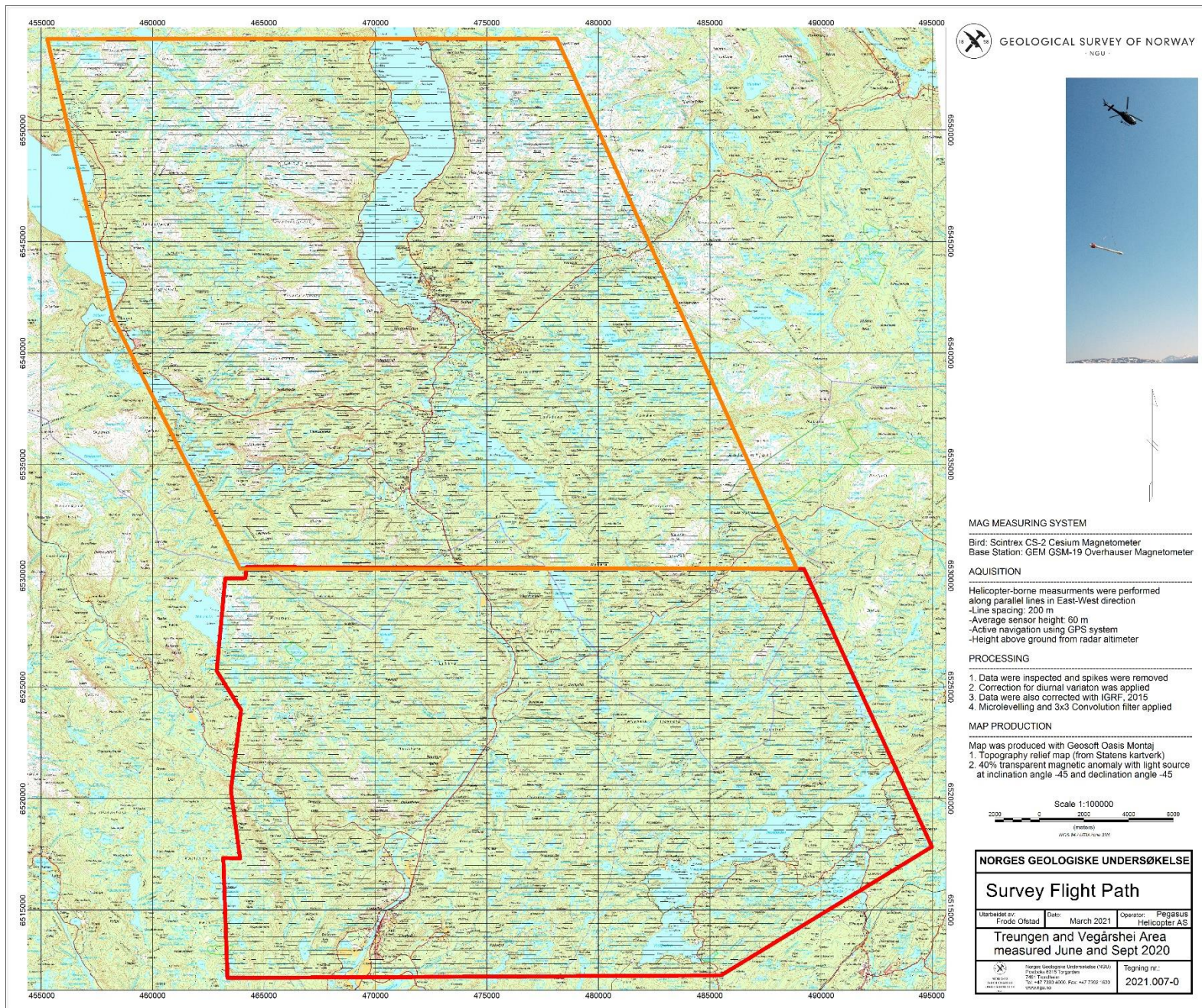


Figure 4: Treungen and Vegårshei survey areas with flight path

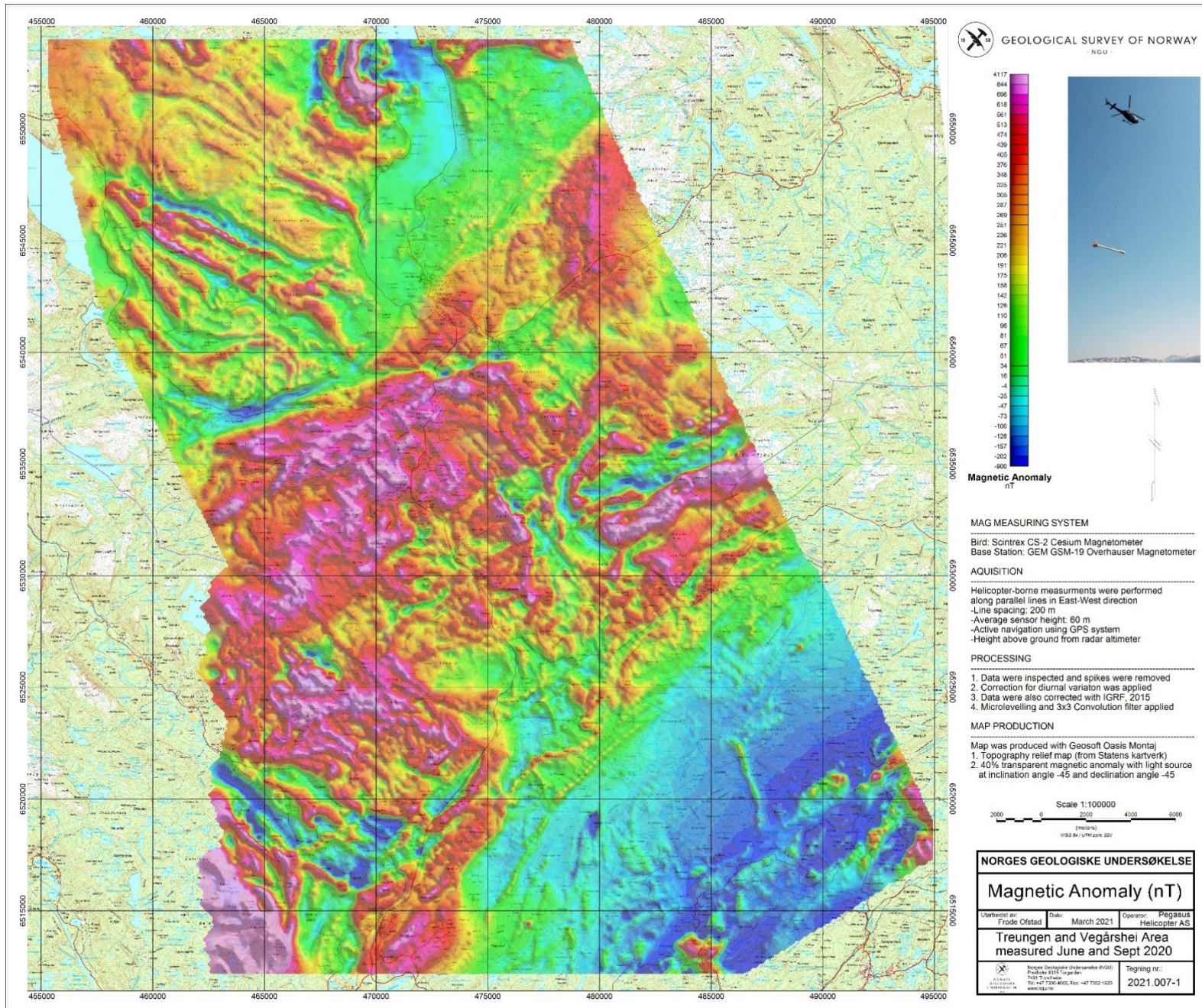


Figure 5: Total Magnetic Field

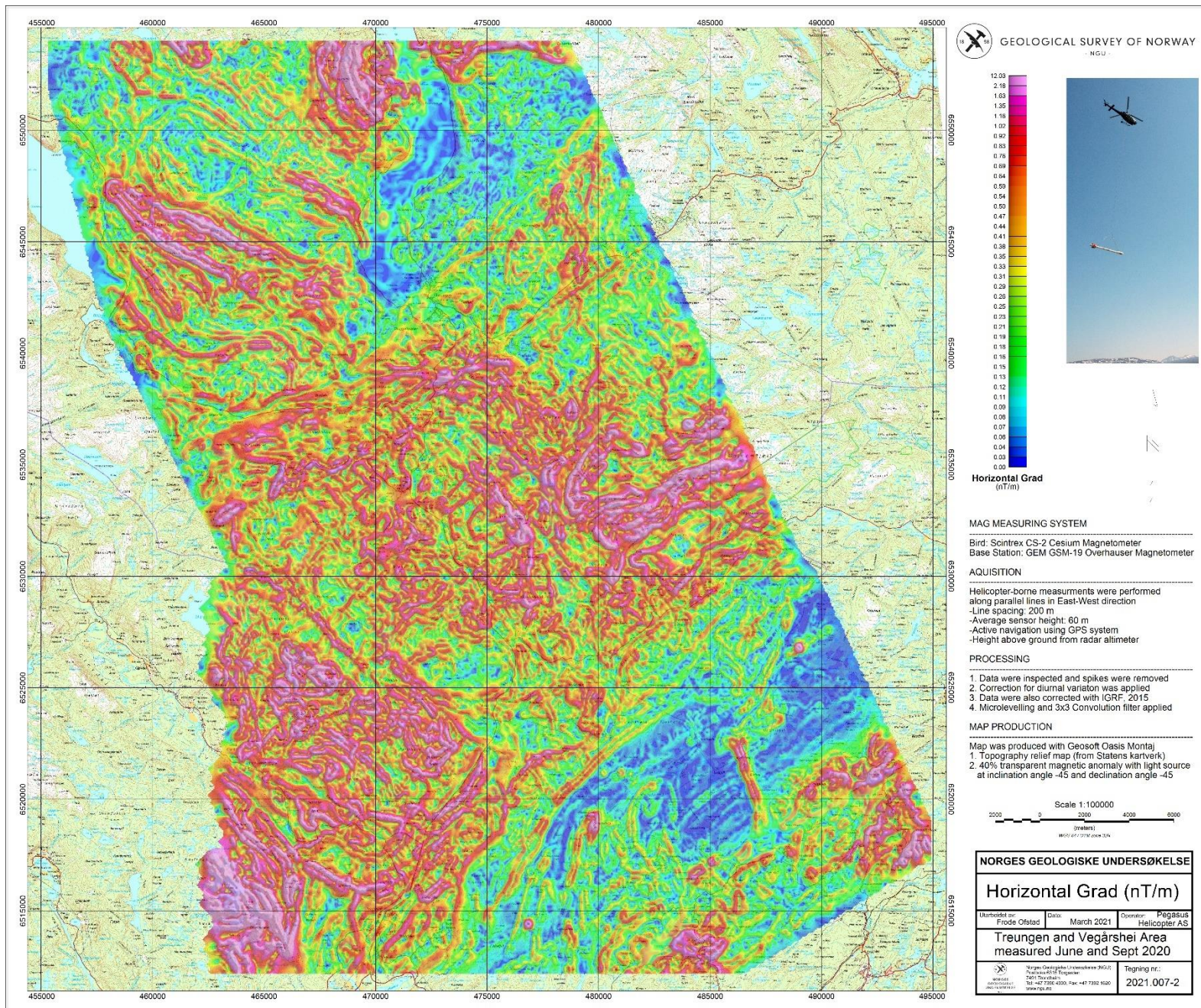


Figure 6: Magnetic Horizontal Gradient

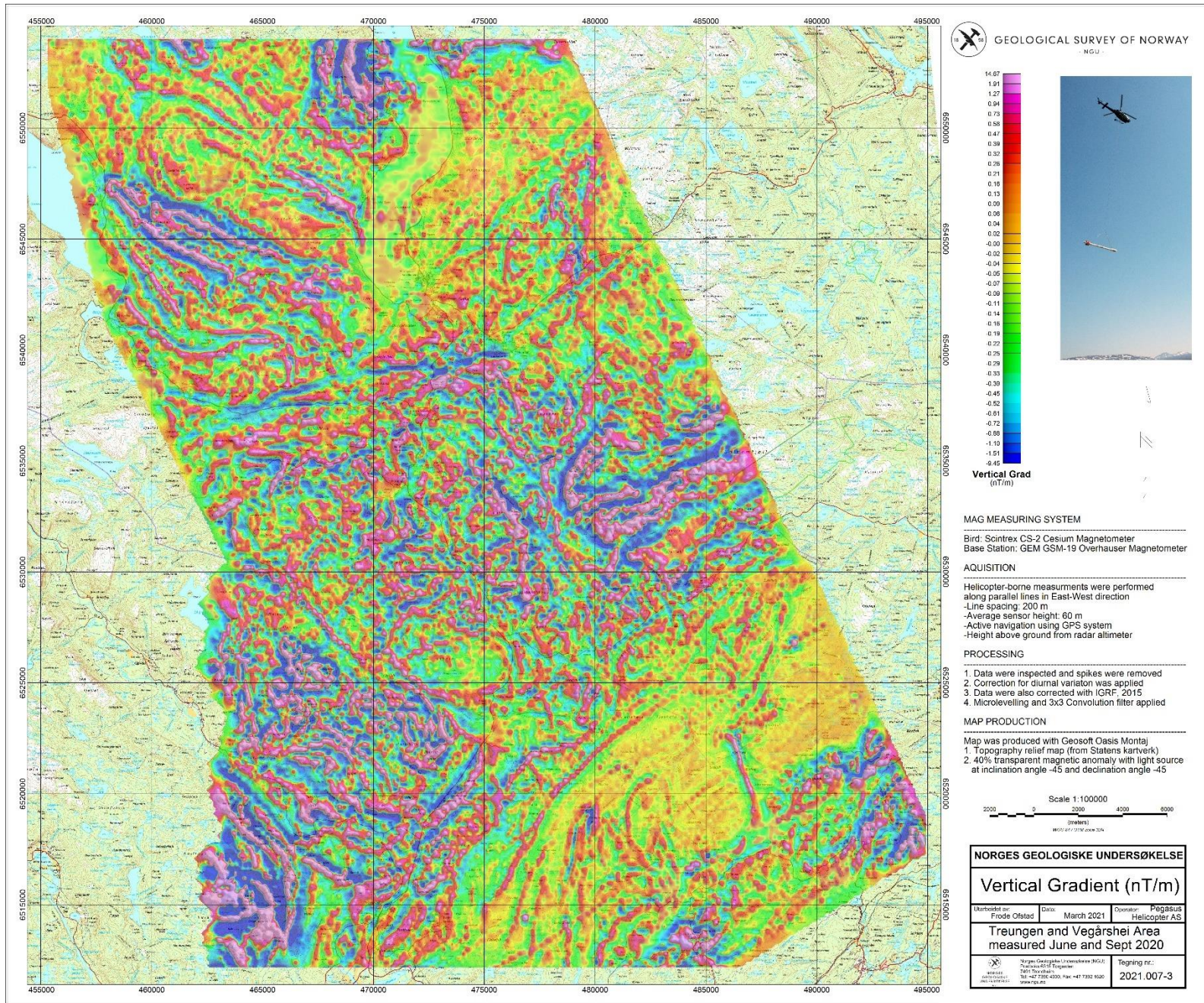


Figure 7: Magnetic Vertical Derivative

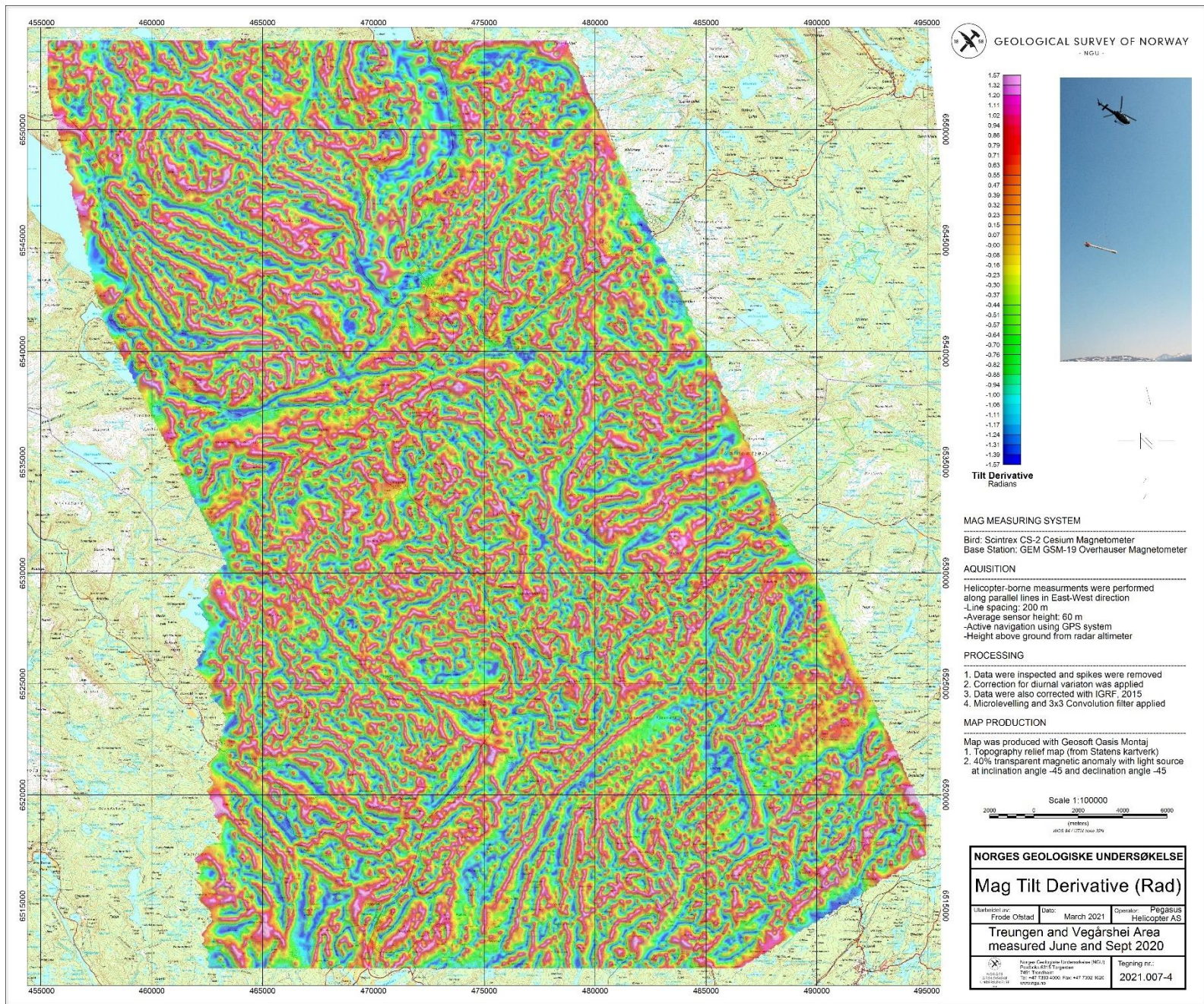


Figure 8: Magnetic Tilt Derivative

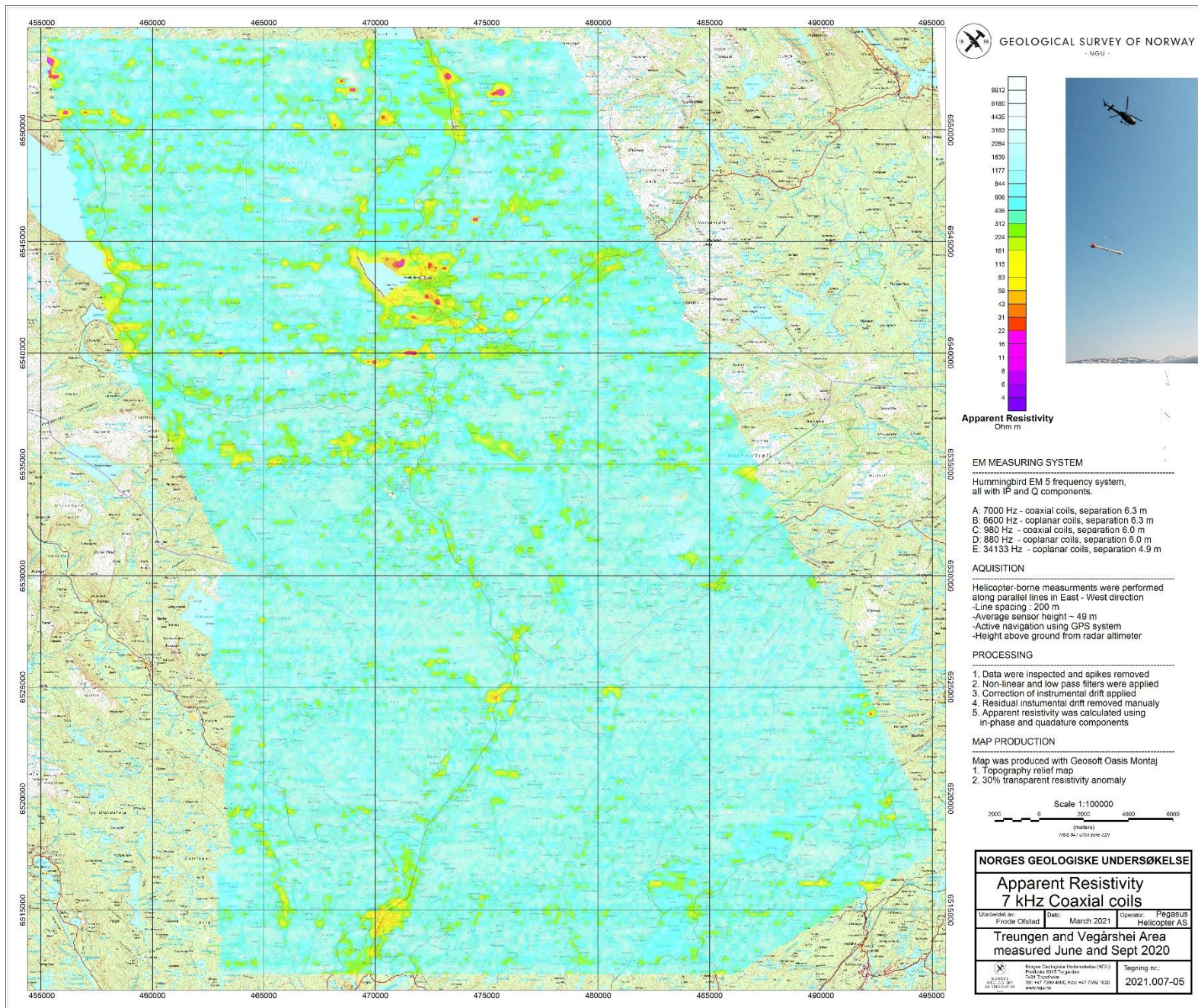


Figure 9: Apparent resistivity. Frequency 7000 Hz, Coaxial coils

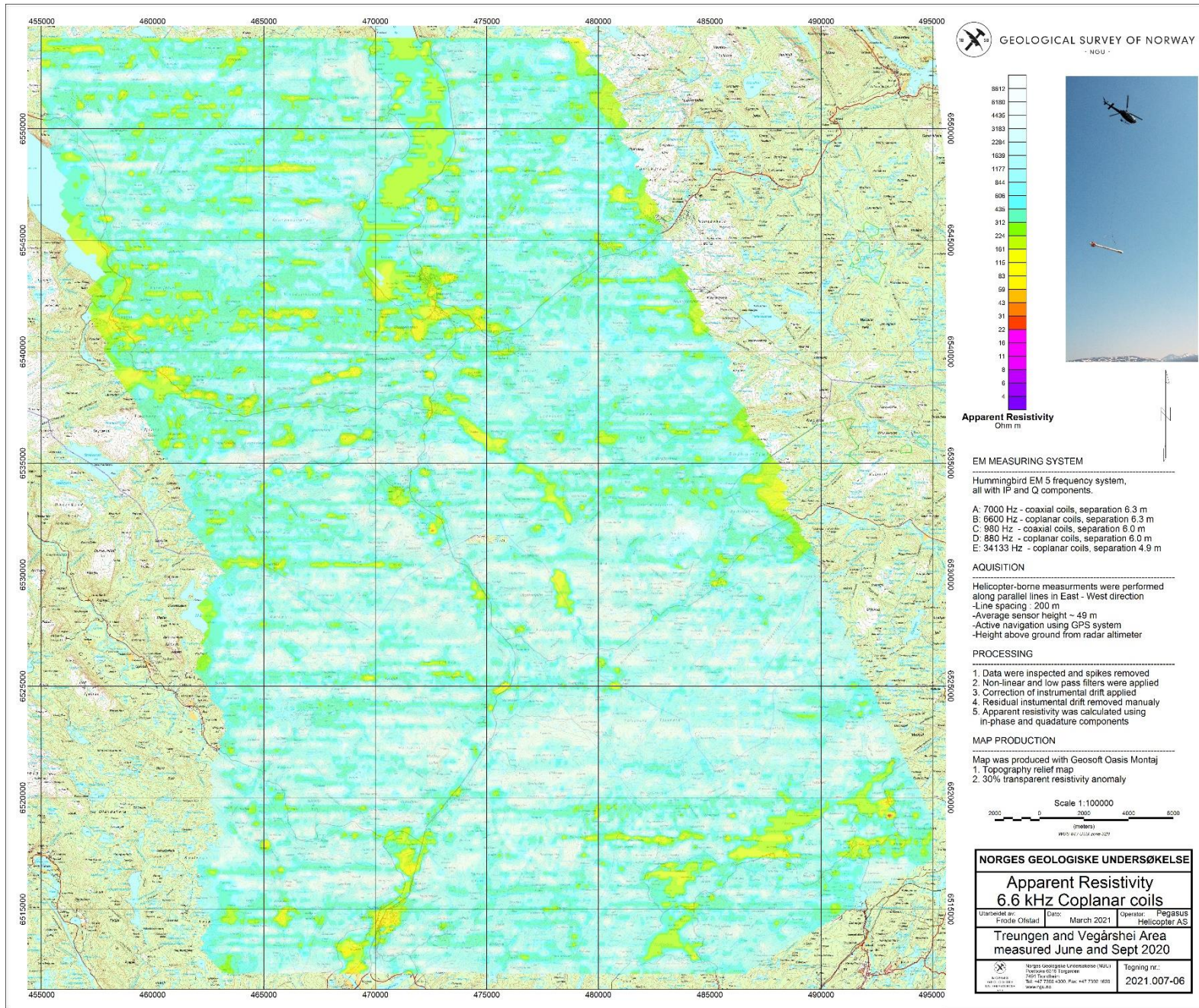


Figure 10: Apparent resistivity. Frequency 6600 Hz, Coplanar coils



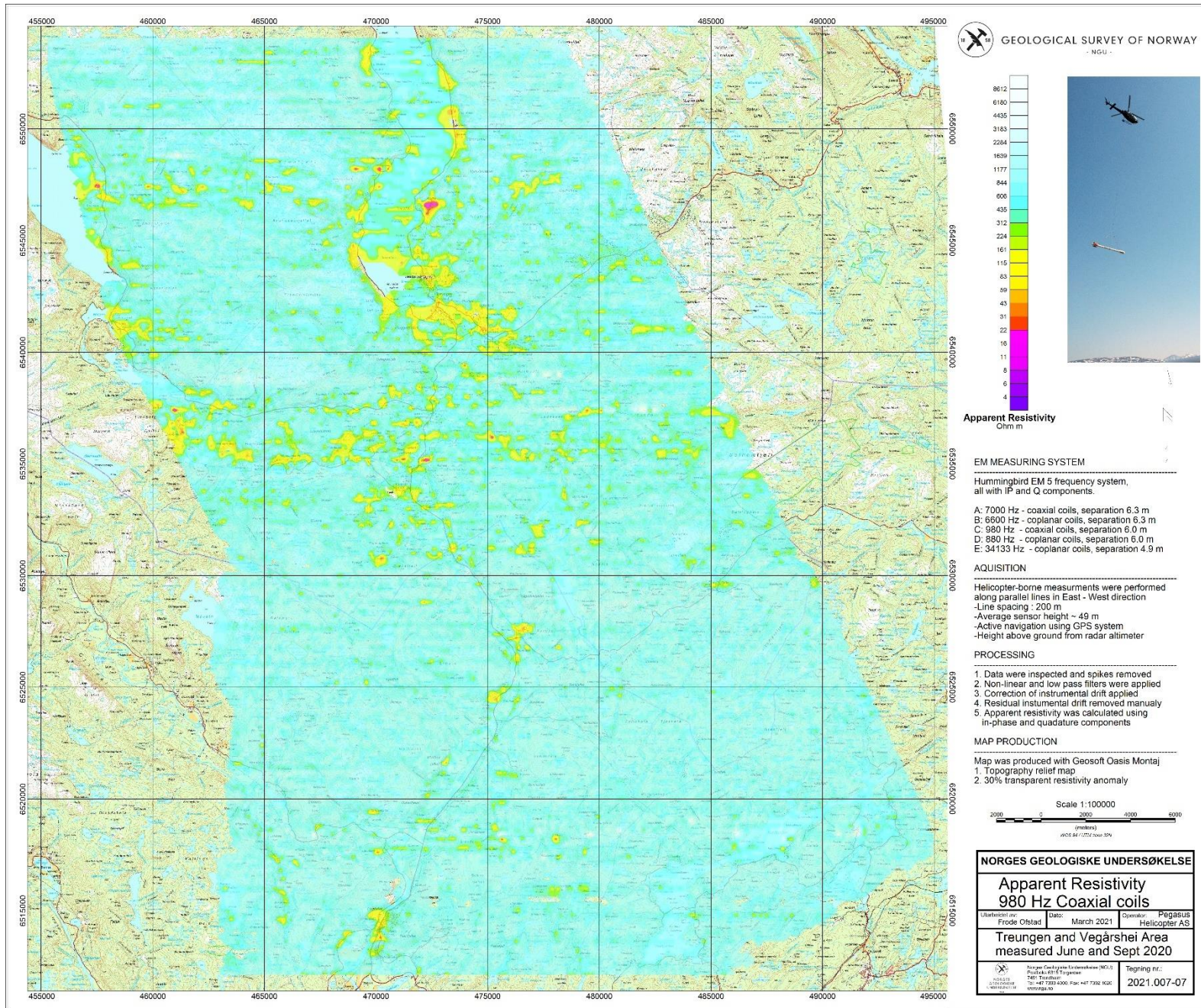


Figure 11: Apparent resistivity. Frequency 980 Hz, Coaxial coils

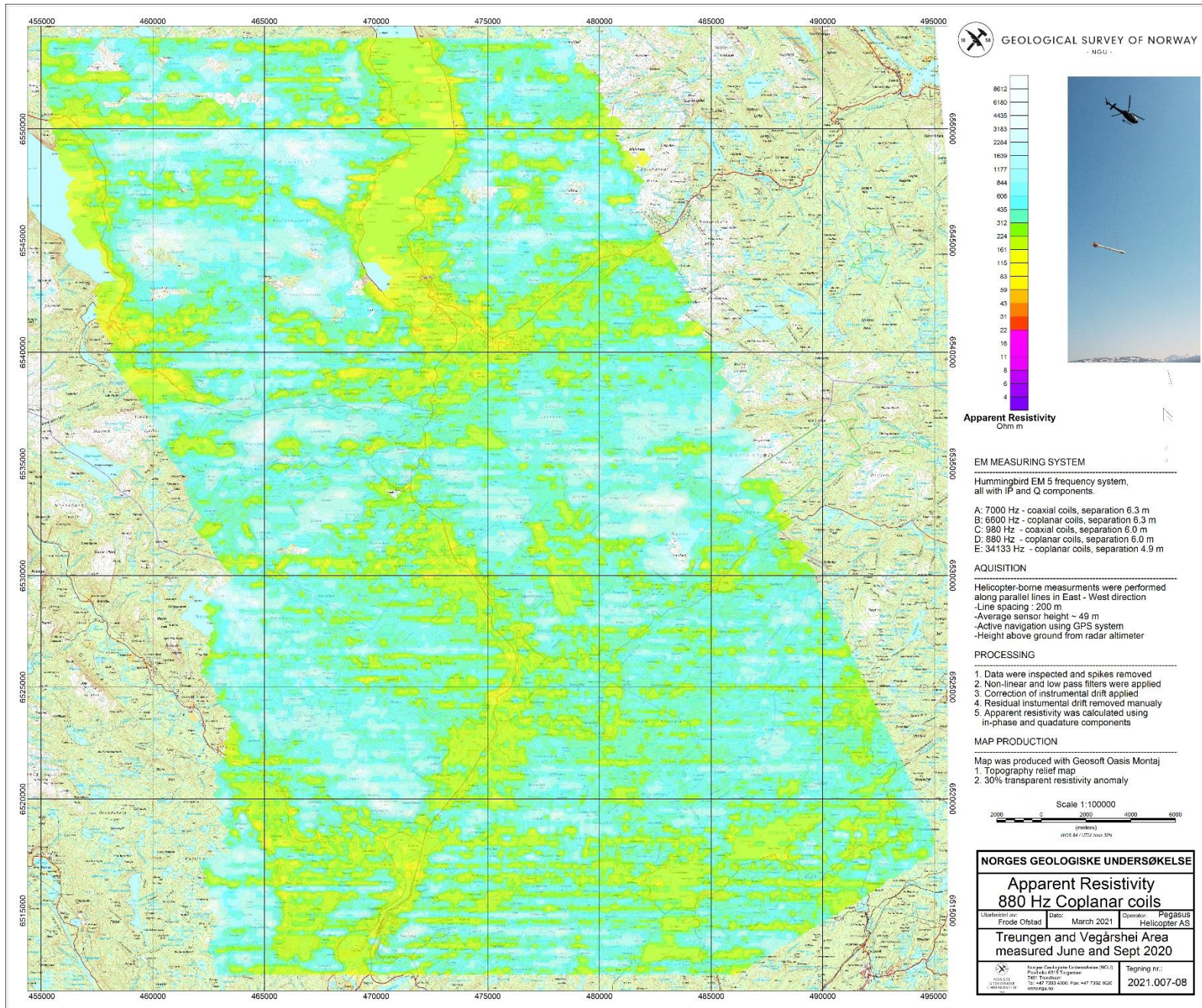


Figure 12: Apparent resistivity. Frequency 880 Hz, Coplanar coils

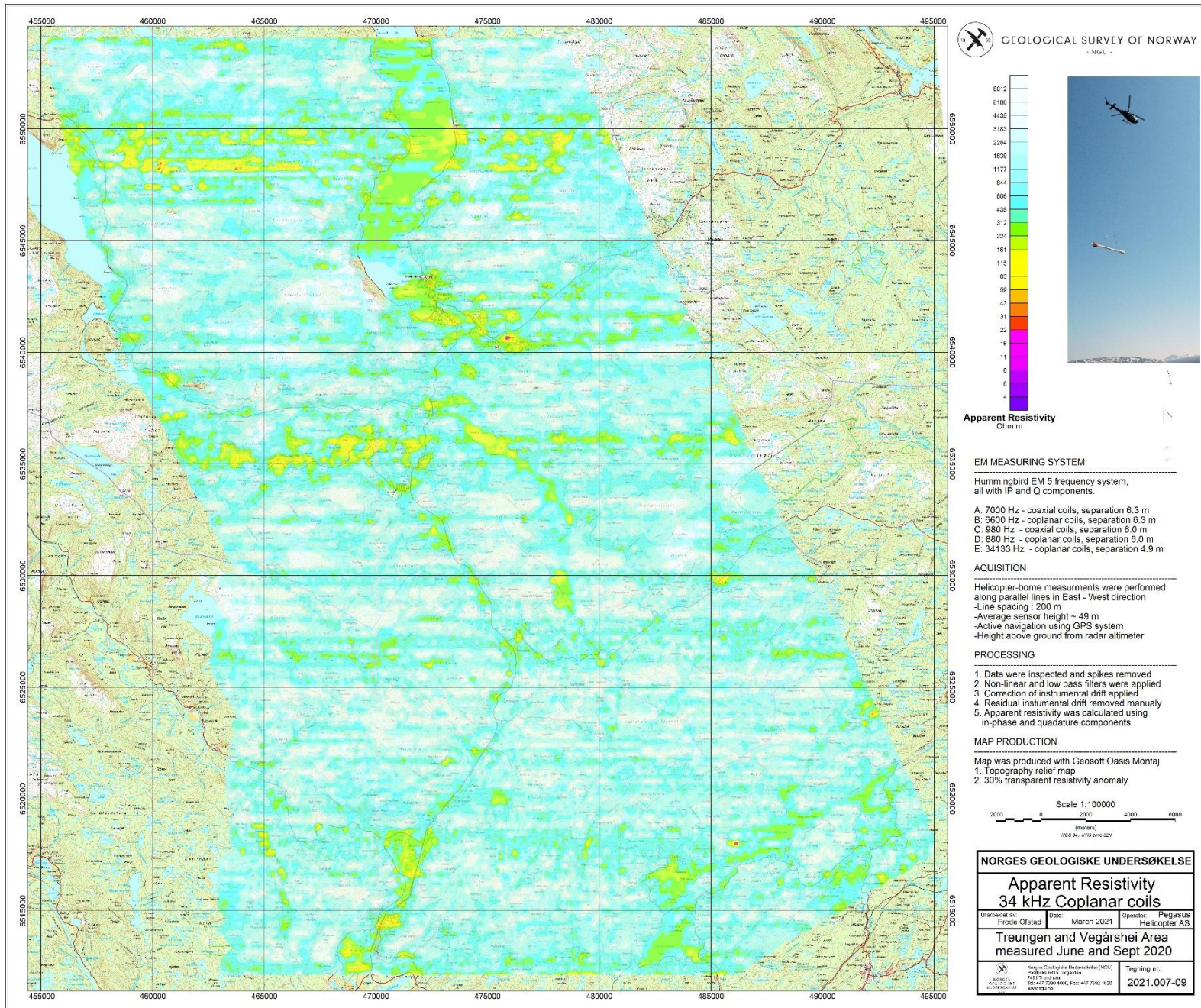


Figure 13 Apparent resistivity. Frequency 34133 Hz, Coplanar coils

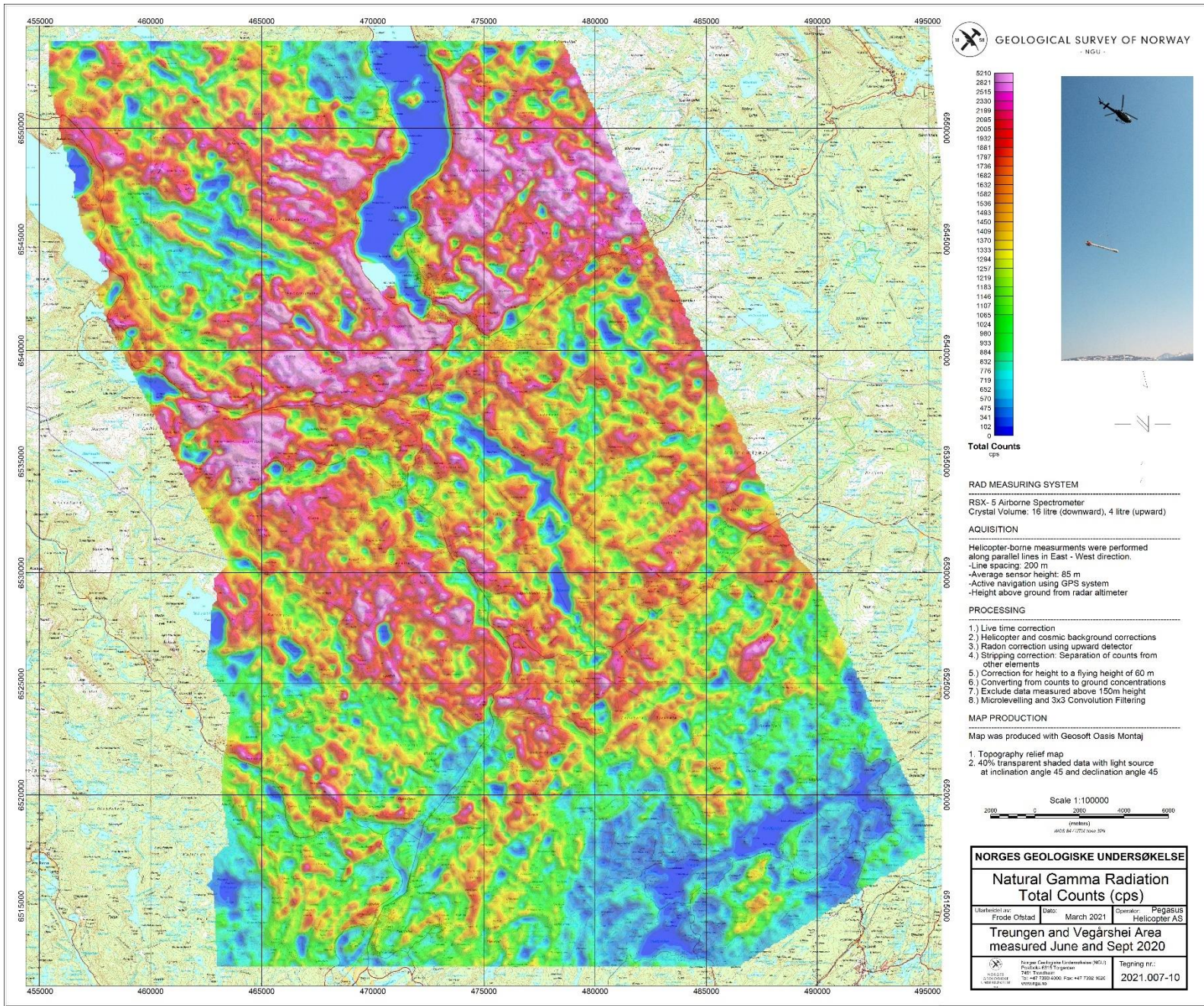


Figure 14: Radiometric Total counts

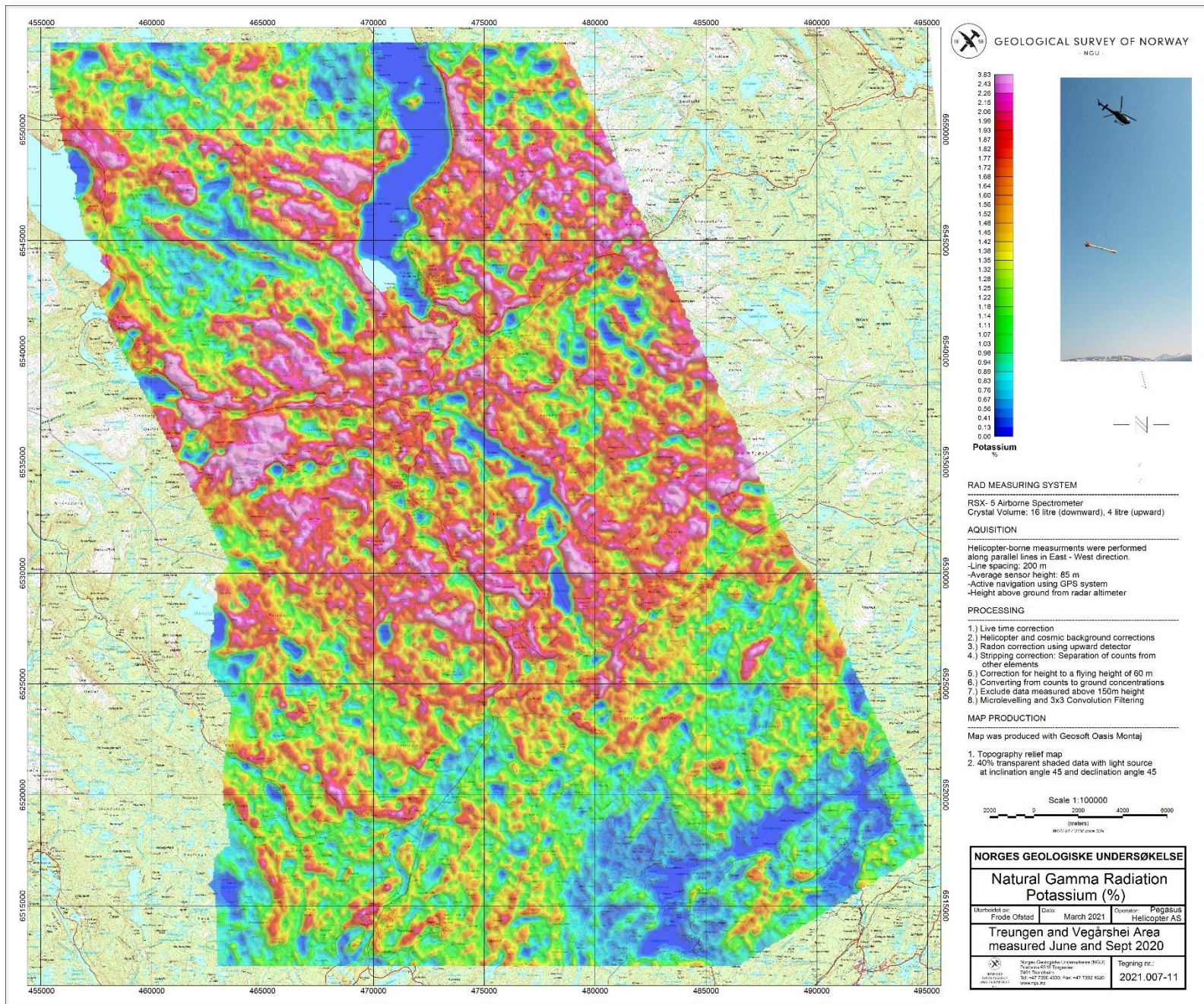


Figure 15: Potassium ground concentration

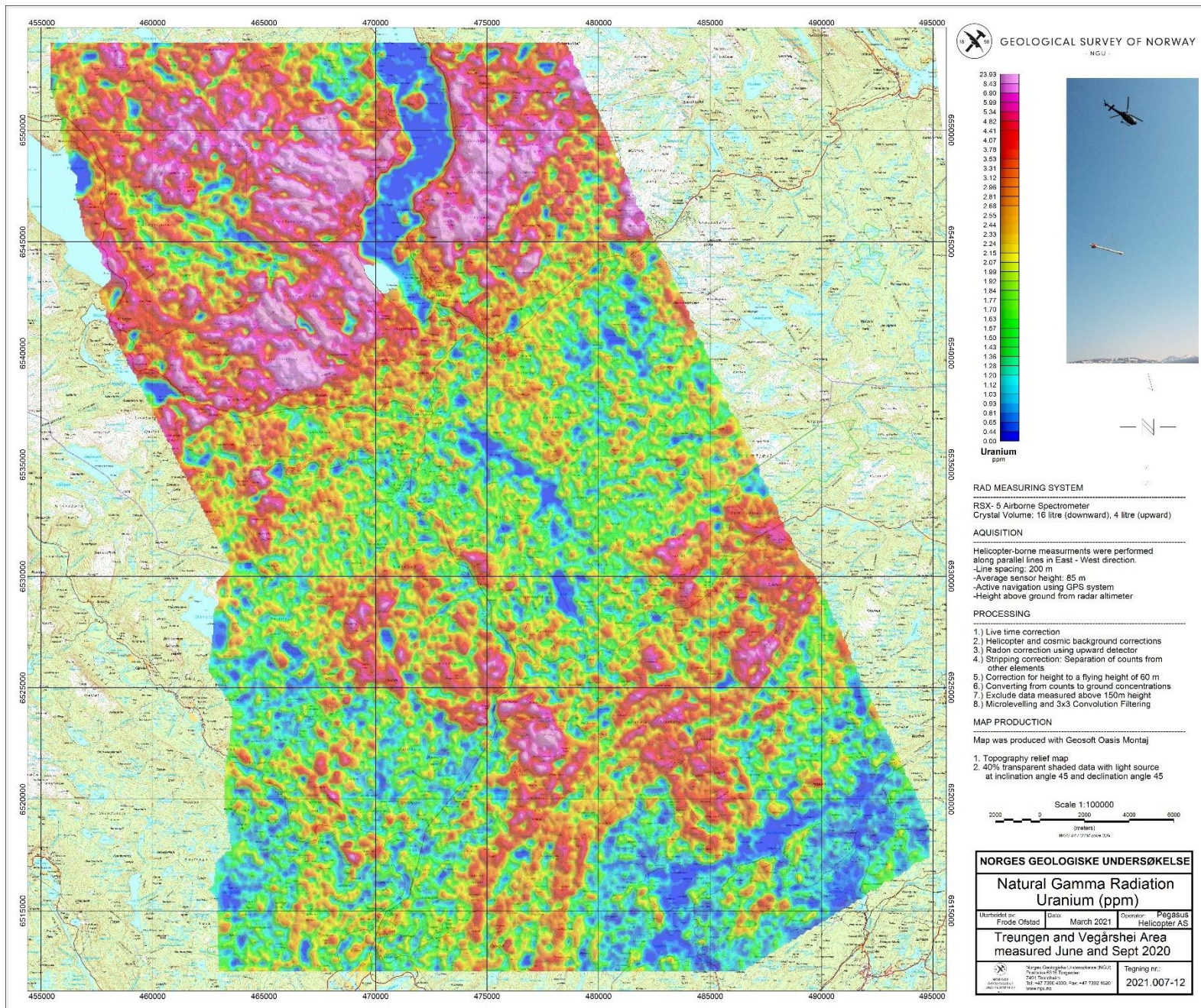


Figure 16: Uranium ground concentration

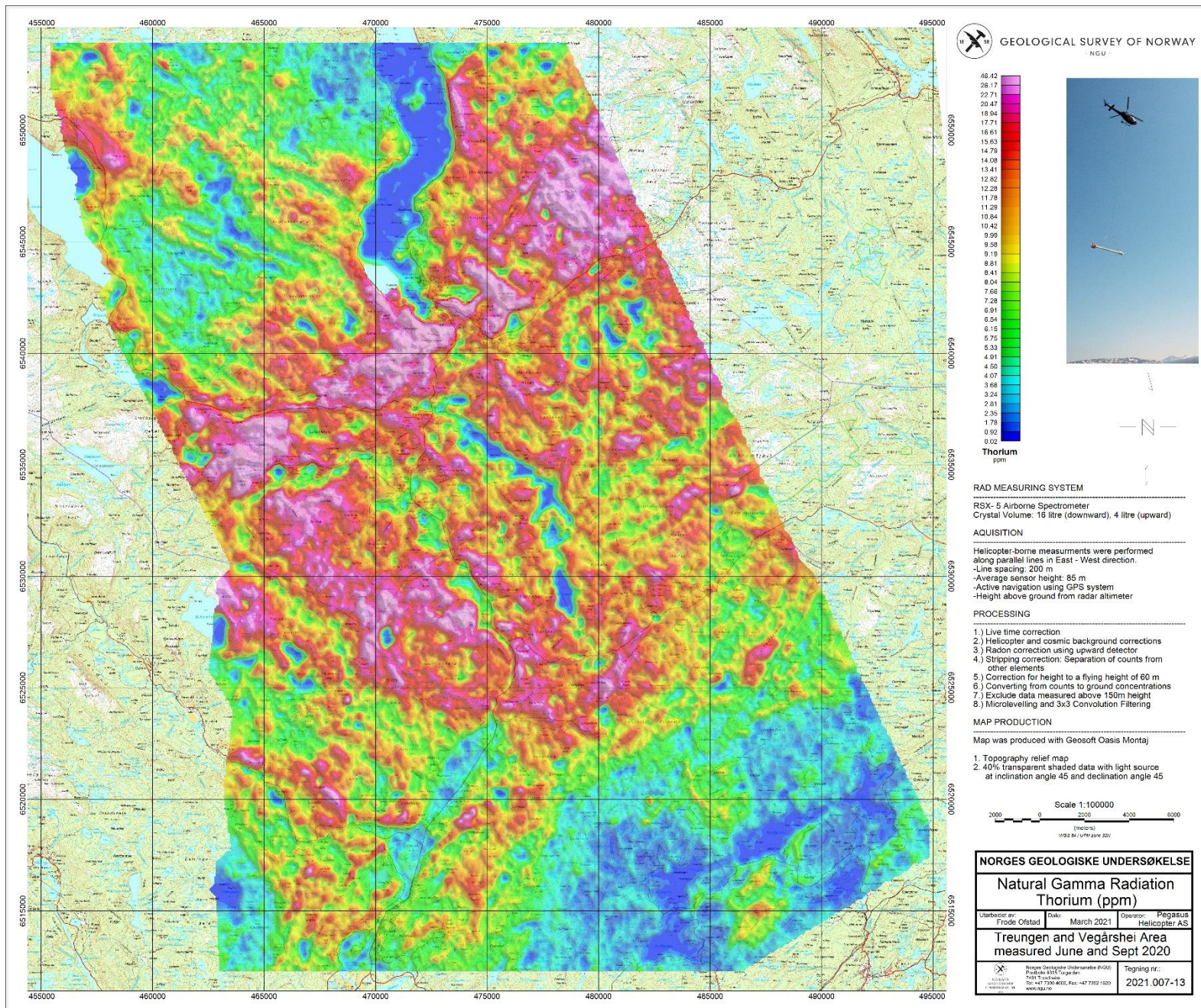


Figure 17: Thorium ground concentration

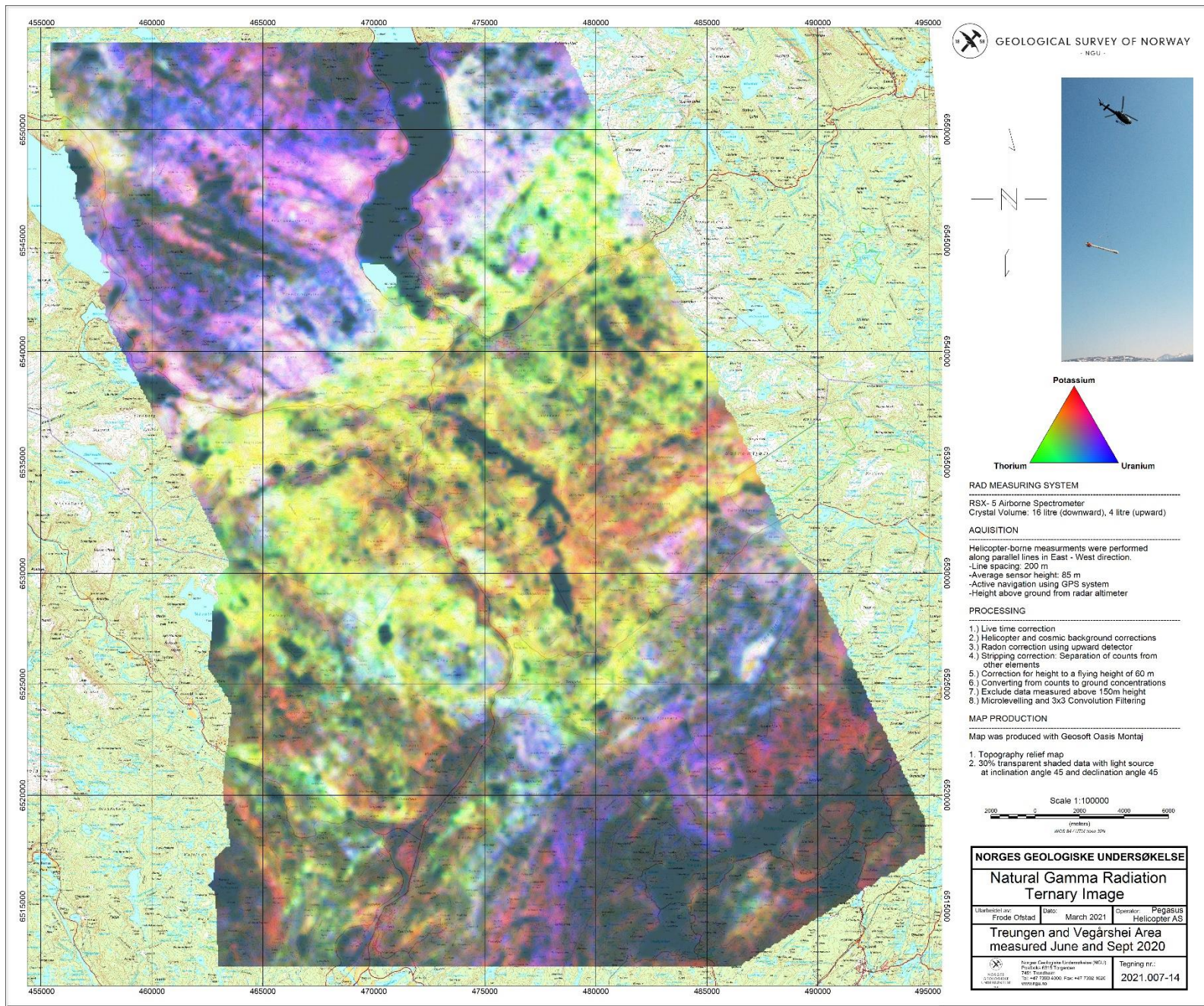


Figure 18: Radiometric Ternary Image





GEOLOGICAL  
SURVEY OF  
NORWAY

· NGU ·

Geological Survey of Norway  
PO Box 6315, Sluppen  
N-7491 Trondheim, Norway

Visitor address  
Leiv Eirikssons vei 39  
7040 Trondheim

Tel (+ 47) 73 90 40 00  
E-mail [ngu@ngu.no](mailto:ngu@ngu.no)  
Web [www.ngu.no/en-gb/](http://www.ngu.no/en-gb/)